High-Performance Crystal Oscillator Circuits: Theory and Application

ERIC A. VITTOZ, SENIOR MEMBER, IEEE, MARC G. R. DEGRAUWE, MEMBER, IEEE, AND SERGE BITZ

Abstract — **A general theory that allows the accurate linear and nonlinear analysis of any crystal oscillator circuit is presented. It is based on the high Q of the resonator and on a very few nonlimiting assumptions. The special case of the three-point oscillator, that includes Pierce and one-pin circuits, is analyzed in more detail. A clear insight into the linear behavior, including the effect of losses, is obtained by means of the circular locus of the circuit impedance. A basic condition for oscillation and simple analytic expressions are derived in the lossless case for frequency pulling, critical transconductance, and start-up time constant. The effects of nonlinearities on amplitude and on frequency stability are analyzed. As an application, a 2-MHz CMOS oscillator is described, which uses amplitude stabilization to minimize power consumption and to eliminate the effects of nonlinearities on frequency. The chip, implemented in a 3-μm p-well low-voltage process, includes a three-stage frequency divider and consumes 0.9 μA at 1.5 V. The measured frequency stability is 0.05 ppm/V in the range 1.1–5 V of supply voltage. Temperature effect on the circuit itself is less than 0.1 ppm from −10 to +60°C.**

I. Introduction

STARTING in the late sixties, large efforts have been devoted to the development of high-performance integrated quartz crystal oscillators for electronic watches. This application requires high stability (1 second per day corresponds to 12 ppm) and very low power consumption, typically 0.1 to 1 μW. Because of the very special domain, few results have been published, most of them in very limited circles [1]–[13]. A more general interest for the problem arose later, for the realization of time bases in microprocessors and switched-capacitor filters. Special problems that appeared in these applications were discussed in a few publications [14]–[17], but these failed to address the important issues of frequency stability and power minimization. Besides the watch, which is still being improved, high-performance crystal oscillators are required in an increasing number of portable instruments where power is limited and precision is of some concern.

The very high quality factor Q and the need for precision prevent direct numerical computer simulation of a crystal oscillator. In particular, direct time-domain simulation to evaluate nonlinear effects would necessitate the calculation of close to one million periods of oscillation. In Section II of this paper, a very powerful analytic approach based on [11] will be presented. This approach allows the accurate calculation of all linear and nonlinear effects in any crystal oscillator, by taking advantage of the high value of Q. Section III concentrates on the particular structure based on a single active device, which is used in most of the practical realizations. As an example, Section IV describes a high-performance CMOS oscillator developed for advanced watch applications.

Manuscript received September 7, 1987; revised November 30, 1987.
The authors are with Centre Suisse d'Electronique et de Microtechnique, Maladière 71, CH 2000 Neuchâtel 7, Switzerland.
IEEE Log Number 8719478.

II. General Method of Analysis of Quartz Crystal Oscillators

A. Crystal Resonator

A quartz crystal resonator may be represented by its electrical equivalent circuit shown in Fig. 1 [18]. Each possible mode (i) of mechanical oscillation corresponds to a series resonant circuit $L(i)$, $C(i)$, $R(i)$ having a motional impedance $Z_m(i)$. The current $i(i)$ through $Z_m(i)$ is proportional to the velocity, thus its amplitude is proportional to the amplitude of oscillation at mode (i). The motional capacitance $C(i)$ is proportional to the electromechanical coupling of mode (i). Since this coupling is always very small, the total capacitance across the main electrodes 1 and 2

$$C_0 = C_{12} + \frac{C_{10} \cdot C_{20}}{C_{10} + C_{20}} \tag{1}$$

is always much larger than $C(i)$. Part of this capacitance is shielded by a third electrode 0, usually connected to the case. Each mode of oscillation may be characterized by its mechanical resonant (angular) frequency (1 and 2 short-circuited)

$$\omega_m(i) = [L(i)C(i)]^{-1/2} \tag{2}$$

and by its quality factor

$$Q(i) = 1/[\omega_m(i)C(i)R(i)]. \tag{3}$$

In most practical resonators, the frequencies of the various modes are not exact multiples of each other, or the undesired modes are very weakly coupled. Thus, when oscillation occurs at a given single mode characterized by L, C, R, Z_m, Q, ω_m, and i, all other series branches may

0018-9200/88/0600-0774$01.00

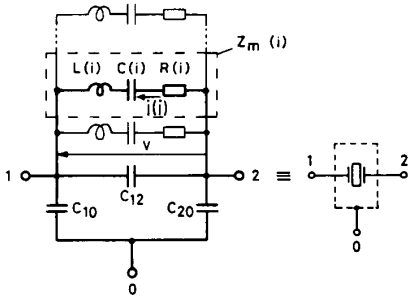

Fig. 1. Equivalent circuit of a crystal resonator.

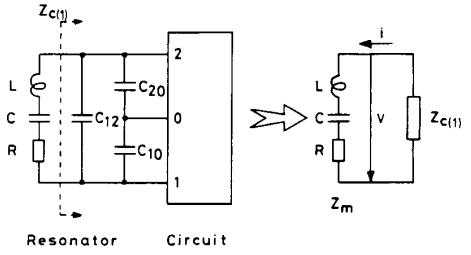

Fig. 2. Most general form of a crystal oscillator. Deep insight and precise analysis are possible by splitting the circuit-resonator combination (a) into the motional impedance Z_m and an equivalent impedance of the circuit at fundamental frequency $Z_{c(1)}$ as shown in (b).

be neglected, even if the voltage v across the device contains large harmonic components. Furthermore, Q is always very large; the current i through the motional impedance Z_m is therefore sinusoidal for any shape of voltage v. The motional impedance may be expressed as

$$Z_m = R + \frac{j}{\omega_m C}\left(\frac{\omega}{\omega_m} - \frac{\omega_m}{\omega}\right). \tag{4}$$

In an oscillator, ω is always very close to ω_m, thus

$$p = \frac{\omega - \omega_m}{\omega_m} \ll 1 \tag{5}$$

which yields

$$Z_m = R + j\frac{2p}{\omega C} \tag{6}$$

where p is the relative amount of frequency pulling above the mechanical resonant frequency ω_m of the resonator.

The mechanical energy of oscillation is given by

$$E_m = \frac{L|I|^2}{2} = \frac{|I|^2}{2\omega^2 C} \tag{7}$$

and the mechanical power dissipation is

$$P_m = \frac{R|I|^2}{2} = \frac{|I|^2}{2\omega Q C} \tag{8}$$

where $|I|$ is the amplitude of sinusoidal current i.

B. Optimum Splitting of the Oscillator

A crystal oscillator is obtained by connecting the three poles of the resonator to an oscillator circuit, as shown in Fig. 2(a). The traditional analysis includes the whole resonator as a component of the circuit [18]–[20]. However, much more insight can be obtained by splitting the oscillator into the linear motional impedance Z_m and the rest of the circuit, which includes capacitances C_{10}, C_{12}, and C_{20} of the resonator and all the nonlinearities.

As was pointed out above, the current through Z_m can be assumed to be *always sinusoidal*, even if voltage v across it is strongly distorted. As a consequence, exchange of energy with the circuit can only occur at the fundamental frequency, and the nonlinear circuit can be completely characterized (Fig. 2(b)) by its equivalent impedance at this frequency

$$Z_{c(1)} = -\frac{V_{(1)}}{I} \tag{9}$$

where $V_{(1)}$ is the complex value of the *fundamental* component of v, which depends on the amplitude of I. Furthermore, since $Z_{c(1)}$ usually has no high-Q pole in the vicinity of ω_m, its frequency dependence is orders of magnitude smaller than that of Z_m. *The frequency ω may therefore be considered constant* (and equal to ω_m) *with regard to $Z_{c(1)}$*, whereas the frequency dependence of Z_m is expressed by means of pulling p, according to (6). These assumptions do not introduce any significant loss of accuracy. They greatly simplify the linear and nonlinear analysis of any crystal oscillator.

C. Linear Analysis

As long as the amplitude of oscillation is small, the whole circuit stays linear, and the impedance $Z_{c(1)}$ reduces to the small-signal impedance Z_c. The critical condition for oscillation can then be simply expressed as

$$Z_c + Z_m = 0. \tag{10}$$

Using expression (6) of Z_m, it can be split into two conditions for the real and imaginary components:

$$-\mathrm{Re}(Z_c) = R \tag{11}$$

shows that the negative resistance of Z_c must exactly compensate the positive resistance R of the resonator; and

$$-\mathrm{Im}(Z_c) = \frac{2p}{\omega C} \tag{12}$$

shows that the amount of frequency pulling p is proportional to the imaginary part of Z_c. As soon as $-\mathrm{Re}(Z_c)$ becomes larger than R, oscillation builds up exponentially from noise, with a time constant

$$\tau = -\frac{L}{\mathrm{Re}(Z_c) + R} = -\frac{1}{\omega^2 C(\mathrm{Re}(Z_c) + R)}. \tag{13}$$

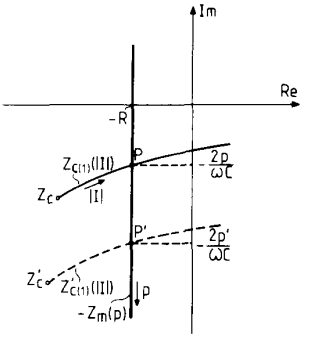

Fig. 3. Locus of $Z_{c(1)}(|I|)$ in the complex plane. It starts at linear impedance Z_c for small amplitude $|I|$. Stable oscillation is reached at intersection P with locus of $-Z_m(p)$.

The time required for growing of oscillation, which depends on the noise level, is usually comprised between 5 and 15τ. It can be reduced by providing more initial energy through an adequate switching procedure [17]. Above a certain level, the circuit becomes nonlinear, which provides amplitude limitation.

D. Nonlinear Behavior and Analysis

When voltage v is distorted by nonlinearities in the circuit, relations (10)–(13) are still applicable, provided the small signal impedance Z_c (which has no more meaning) is replaced by the impedance for the fundamental component of voltage $Z_{c(1)}$ defined by (9). As is shown qualitatively in the complex plane of Fig. 3, the increasing rate of distortion due to an increase of amplitude $|I|$ progressively reduces the value of $-\mathrm{Re}(Z_{c(1)})$, which is the negative resistance provided by the circuit, until stable oscillation is reached for

$$Z_{c(1)} + Z_m = 0. \tag{14}$$

This occurs when the locus of $Z_{c(1)}(|I|)$ intercepts the locus of $-Z_m(p)$ at point P. The exact values of frequency pulling p and amplitude of oscillation are then given, respectively, by the imaginary part of Z_m (according to (6)) and by the value of $|I|$ at point P.

An accurate numerical simulation of the nonlinear behavior of any crystal oscillator can thus be carried out in the following manner. For a given circuit configuration, with given bias conditions, the impedance $Z_{c(1)}$ can be calculated by time simulation for a given amplitude $|I|$: the sinusoidal current i (complex value I) is imposed by a current source, and the resulting periodic voltage v is computed. Its complex fundamental component $V_{(1)}$ is then extracted by Fourier analysis and divided by I, according to (9). The locus of $Z_{c(1)}(|I|)$ is obtained by repeating this procedure for increasing values of $|I|$.

This kind of amplitude limitation by distortion has many disadvantages. As shown by the dotted curve in Fig. 3, any change in the circuit bias (due for instance to a variation of supply voltage or temperature) corresponds to a new value of small signal impedance Z_c', a new locus

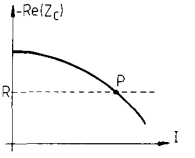

Fig. 4. Ideal nondistorting amplitude limitation.

$Z'_{c(1)}(|I|)$, and a new stable point P', with a new value p' of frequency pulling. The frequency stability can therefore be strongly degraded. Furthermore, such a limitation has a poor power efficiency, since a large part of the supply power is wasted in producing harmonics. It also complicates the selection of the desired mode (i) of oscillation of the resonator [11].

In high-performance oscillators, these problems must be eliminated by limiting the amount of distortion. Fixing the bias point just above the critical condition for oscillation would not leave enough margin for variations in the process, neither in the resonator nor in the environment. The solution consists in using a feedback loop, with a time constant much larger than the period of oscillation. As illustrated in Fig. 4 in an ideal case with no distortion, such a regulator reduces $-\mathrm{Re}(Z_c)$ (usually by reducing the bias current) when the amplitude $|I|$ increases, until equilibrium is reached at point P. In practice, the stable amplitude at point P is chosen low enough to avoid any significant distortion, so that the circuit operates very close to the critical condition for oscillation.

III. Theory of the Three-Point Oscillator

A. General Linear Circuit

Excellent oscillators can be implemented by using essentially a single transconductance device, such as a bipolar or a MOS transistor [18], [19]. It can be shown that, since no integrated inductor is available, the only possibility is to associate the transconductance with two functional capacitors, to form the three-point oscillator shown in Fig. 5. The most general form of this oscillator, after separation of the motional impedance Z_m, is represented by its ac diagram in Fig. 6. Impedances $Z_1 - Z_3$ include all the components of the real active device, except its transconductance g_m, and all other possible contributions. As discussed previously, their values can be considered constant (independent of frequency pulling $p \ll 1$) without any significant loss of accuracy. The small-signal circuit impedance is easily obtained as

$$Z_c = \frac{Z_1Z_3 + Z_2Z_3 + g_mZ_1Z_2Z_3}{Z_1 + Z_2 + Z_3 + g_mZ_1Z_2}. \tag{15}$$

This relation is a bilinear function of g_m. Therefore, the locus of $Z_c(g_m)$ in the complex plane is a circle (half-circle for $0 < g_m < \infty$) as shown in Fig. 7. This circle is always located inside the lower half-plane, since the reactive components are all capacitive.

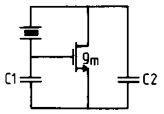

Fig. 5. Basic three-point oscillator.

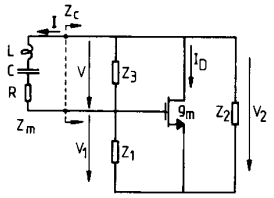

Fig. 6. General form of the three-point oscillator.

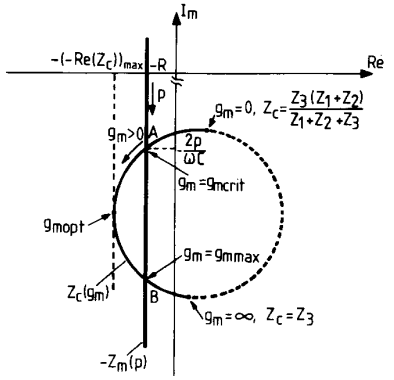

Fig. 7. Complex plane representation of the general three-point oscillator (linear). Stable critical oscillation corresponds to intersection A of loci $Z_c(g_m)$ and $-Z_m(p)$.

The critical conditions for oscillation correspond to intersections A and B of this locus with that of $-Z_m(p)$. It can be shown that no stable oscillation is possible at point B, because the phase stability condition [21] is not satisfied. The critical transconductance for oscillation $g_{m\,\mathrm{crit}}$ may thus be calculated by introducing (15) into (11) and selecting the smaller solution (point A) for g_m. The second solution is $g_{m\,\max}$ (point B), beyond which no oscillation can start, as was pointed out elsewhere [15].

The negative resistance $-\mathrm{Re}(Z_c)$ provided by the circuit reaches a maximum for an intermediate value $g_{m\,\mathrm{opt}}$ of transconductance. If resistance R in the motional impedance is larger than this maximum value, no oscillation is possible, whatever the value of the transconductance. If oscillation is possible, the start-up time constant given by (13) reaches a minimum for $g_m = g_{m\,\mathrm{opt}}$. The representation of Fig. 7 also allows one to predict the qualitative influence of the three circuit impedances on frequency pulling p. An increase of the imaginary part of Z_1 or Z_2 (reduction of C_1 or C_2) reduces the diameter of the circle and always moves the stable point A downwards, which causes an increase of p. An increase of the imaginary part of Z_3 (reduction of C_3) moves the whole circle downwards and increases its diameter. As a result, point A may move downwards or upwards, depending on its initial position.

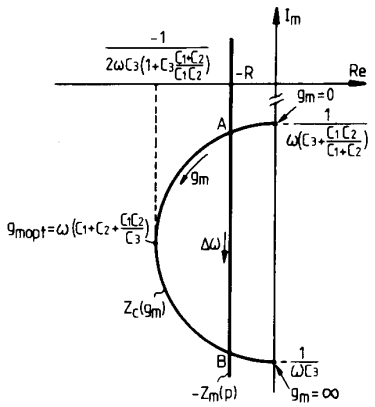

Fig. 8. Complex plane representation of the lossless three-point oscillator (linear).

Any increase of the real part of Z_1, Z_2, or Z_3 moves the circle to the right, and causes an increase of p by pushing A downwards. These real parts correspond to losses in the circuit. They can be due to losses in the active device (output conductance, input conductance for a bipolar), to the components that must be added to bias it in active mode, to the external load of the oscillator, and to parasitic effects such as interconnection resistance or moisture.

B. Lossless Linear Circuit

Losses in the circuit should be minimized to achieve minimum critical transconductance (and thus minimum current for oscillation) and maximum frequency stability. The ideal case with purely capacitive impedances (no other losses than that of the resonator) corresponds to the complex plane representation of Fig. 8. The real and imaginary parts of Z_c are then

$$\mathrm{Re}(Z_c) = -\frac{g_m C_1 C_2}{(g_m C_3)^2 + \omega^2 (C_1 C_2 + C_2 C_3 + C_3 C_1)^2} \tag{16}$$

$$\mathrm{Im}(Z_c) = -\frac{g_m^2 C_3 + \omega^2 (C_1 + C_2)(C_1 C_2 + C_2 C_3 + C_3 C_1)}{\omega\left[(g_m C_3)^2 + \omega^2 (C_1 C_2 + C_2 C_3 + C_3 C_1)^2\right]}. \tag{17}$$

The maximum negative resistance is obtained for

$$g_m = g_{m\,\mathrm{opt}} = \omega\left(C_1 + C_2 + \frac{C_1 C_2}{C_3}\right) \tag{18}$$

and has the value

$$(-\mathrm{Re}(Z_c))_{\max} = \frac{1}{2\omega C_3\left(1 + \dfrac{C_1 + C_2}{C_1 C_2} C_3\right)} \tag{19}$$

which must be larger than resistance R to allow oscillation. By using (3), this condition can be expressed as

$$\frac{QC}{C_3} > 2\left(1 + C_3 \frac{C_1 + C_2}{C_1 C_2}\right). \tag{20}$$

As seen in Fig. 8, the imaginary part of Z_m at the stable point A is a function of its real part R. The frequency pulling p therefore depends on the quality factor of the resonator, which is quite unsatisfactory for frequency stability. Meanwhile, if condition (20) is fulfilled with a large enough margin, point A stays very close to the imaginary axis, and this dependence is very small. The introduction of (17) with $g_m \to 0$ into (12) yields a value of frequency pulling independent of R and Q:

$$p = \frac{C}{2\left(C_3 + \dfrac{C_1C_2}{C_1 + C_2}\right)}. \tag{21}$$

Introducing (16) into (11) with the same hypothesis yields the critical transconductance for oscillation:

$$g_{m\,\mathrm{crit}} = \frac{\omega}{QC} \cdot \frac{(C_1C_2 + C_2C_3 + C_3C_1)^2}{C_1C_2}. \tag{22}$$

It can be reduced by reducing capacitor values, at the cost of an increase of p given by (21). This trade-off between transconductance (related to current) and frequency pulling (related to stability) is best expressed by introducing (21) into (22); this yields

$$g_{m\,\mathrm{crit}} = \frac{\omega C}{Qp^2} \cdot \frac{(C_1 + C_2)^2}{4C_1C_2} \tag{23}$$

which is a minimum for $C_1 = C_2$.

The minimum start-up time constant is achieved for the optimum value of transconductance given by (18). It can be obtained by introducing (19) into (13). Neglecting R, this yields

$$\tau_{\min} = \frac{2C_3}{\omega C}\left(1 + \frac{C_1 + C_2}{C_1C_2}C_3\right). \tag{24}$$

The absolute minimum possible for a given resonator is obtained when C_3 is reduced to $C_{12} \ll C_1$ and C_2, which results in

$$\tau_{\mathrm{minmin}} = \frac{2C_{12}}{\omega C}. \tag{25}$$

Because of the small piezoelectric coupling coefficient of quartz material, the value of C_{12}/C is always at least several hundred. Therefore, the start-up time constant always exceeds 100 periods of oscillations, which corresponds to a start-up time that always lies above 1000 periods.

C. Amplitude of Oscillation

When the critical transconductance $g_{m\,\mathrm{crit}}$ is exceeded by applying a dc bias current I_0 to the active device above a critical value $I_{0\,\mathrm{crit}}$, oscillation builds up. Nonlinear effects start appearing when the amplitude $|V_1|$ of the sinusoidal driving voltage of the device (see Fig. 6) becomes so large as to generate harmonics in its output current i_D. The small-signal transconductance must then be replaced by the transconductance for the fundamental defined as

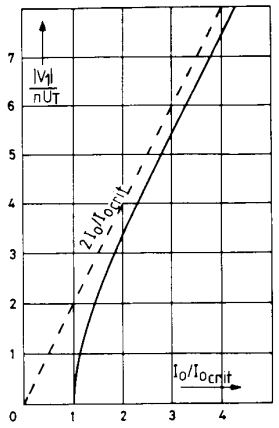

Fig. 9. Amplitude of oscillation for an active device with exponential transfer characteristics.

$$g_{m(1)} = \frac{I_{D(1)}}{V_1} \tag{26}$$

which is still real, since the fundamental component $I_{D(1)}$ of i_D is in phase with V_1. Amplitude $|V_1|$ stops increasing when $g_{m(1)} = g_{m\,\mathrm{crit}}$, which yields the stable value

$$V_1 = \frac{I_{D(1)}}{g_{m\,\mathrm{crit}}} = \frac{I_{D(1)}}{I_0} \cdot \frac{I_0}{g_{m\,\mathrm{crit}}} \tag{27}$$

where $I_{D(1)}/I_0$ must be calculated by Fourier analysis.

If the active device is a MOS transistor, it should be operated in weak inversion [10], which provides a maximum value of transconductance for a given bias current I_0

$$g_m = \frac{I_0}{nU_T} \tag{28}$$

and exponential transfer characteristics

$$i_D \sim \exp\left(\frac{v_G}{nU_T}\right) \tag{29}$$

where U_T stands for kT/q and n is the slope factor. Taking $|V_1|$ as the amplitude of the sinusoidal component of total gate voltage v_G, the combination of (27) to (29) yields

$$\frac{I_0}{I_{0\,\mathrm{crit}}} = x\frac{I_{B0}(x)}{2I_{B1}(x)} \tag{30}$$

where

$$x = |V_1|/nU_T \tag{31}$$

and I_{B0} and I_{B1} are zero- and first-order modified Bessel functions. This relation is plotted in Fig. 9. It is also valid for a bipolar transistor ($n = 1$). If the MOS transistor is

operated in strong inversion, the amplitude for a given bias current can be shown to be smaller. For very large amplitudes, the transistor only conducts during a very short fraction of the period. For the limit case of Dirac current pulses, $|I_{D(1)}| = 2I_0$ and (27) becomes

$$|V_1| = \frac{2I_0}{g_{m\,\mathrm{crit}}}. \tag{32}$$

This relation gives the maximum possible amplitude which can be obtained with bias current I_0, independently of the shape of the transfer characteristics. It is also reported in Fig. 9.

The maximum power P_m dissipated in the resonator can be evaluated by assuming negligible losses and $C_3 \ll C_1$ and C_2. The current flowing through Z_3 may then be neglected, which gives

$$|I| < \omega C_1 |V_1|. \tag{33}$$

The combination of (8), (22), (32), and (33) results in

$$P_m < \frac{2QC}{\omega C_2^2} I_0^2. \tag{34}$$

The exact value of P_m can be obtained by computing $|I|$ with the method described in Section II-D.

D. Frequency Stability

The frequency stability of a quartz crystal oscillator can be affected by various causes.

Instabilities are first due to the resonator itself. Its natural mechanical frequency usually changes with temperature and aging. Although temperature compensation with the circuit is in principle possible [19], it will not be considered here. The circuit will be required to have a negligible additional effect on stability.

Nonlinearities in the circuit can have a devastating effect on stability, through the mechanisms explained in Section II-D. This can be avoided by limiting the amplitude of oscillation to reduce distortions. If nonlinear effects are limited to the transfer characteristics of the active device, as discussed in Section III-C, a small influence on the frequency of stable oscillation occurs in the following manner. The harmonic components of i_D create harmonics of voltage v_2 across Z_2. Harmonics of current flow through Z_3 and slightly distort driving voltage v_1 across Z_1. These harmonics are then intermodulated in the device nonlinearity, eventually creating an additional fundamental component of i_D with a different phase, which shifts the frequency. If Z_3 were infinite, v_1 would not be distorted and there would be no effect on the frequency. Z_3 should then be as large as possible.

Linear effects on stability can be due to variations of losses, either in the resonator (variation of Q) or in the circuit. Referring to Fig. 7, these can be minimized by ensuring a small slope of the tangent to the circle at equilibrium point A. This requires low losses, large enough values of C_1 and C_2, and a small value of C_3. The remaining instabilities will be due to variations of the capacitances, according to (21). They can be minimized by reducing the nominal frequency pulling p (which costs current, according to (23)) and by minimizing the voltage and temperature sensitivities of the capacitors.

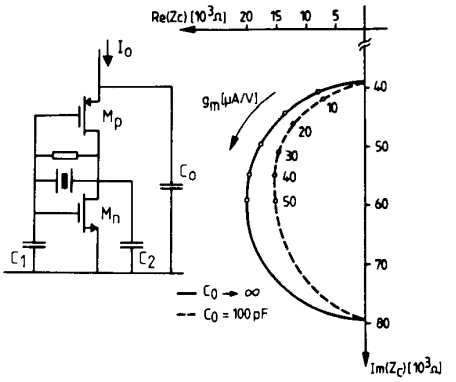

Fig. 10. CMOS inverter oscillator with controlled current. (a) Circuit diagram. (b) Example of locus of $Z_c(g_m)$ for $\omega/2\pi = 2$ MHz, $C_1 = C_2 = 2$ pF, and $C_3 = 1$ pF.

E. Possible Practical Implementations

The various possible implementations of the basic three-point oscillator differ in the choice of the grounded node. Grounding the gate would require two equal bias current sources and is not really feasible. The grounded drain configuration has the advantage of requiring only one additional pin for the resonator [16]. Its major drawback is an increase of C_3 by one of the shielded capacitors C_{10} or C_{20} of the resonator. This reduces the diameter of the circle of Fig. 7 and therefore degrades the frequency stability. The transistor must be placed in a separate well to eliminate bulk modulation, which adds a large voltage-dependent capacitor to C_2 and further deteriorates stability.

The grounded source configuration, also called the Pierce oscillator, is therefore preferred for high-precision oscillators. It is often implemented by means of a CMOS inverter biased in its active region [4], [20]. Because of the inherent class AB operation of the inverter, the current increases with the amplitude of oscillation, which creates very strong nonlinear effects. This results in a very poor frequency stability and a huge waste of power [11]. This solution, which has the advantages of simplicity and rail-to-rail amplitude of oscillation, is only applicable in noncritical situations.

A CMOS inverter with controlled bias current could be implemented as shown in Fig. 10(a). The advantage would be to add the transconductances of the complementary devices which are biased by the same current. This requires the source of M_p to be grounded for ac signals with capacitors C_0. Since C_0 cannot be infinite, Z_c is no longer a bilinear function of g_m, and the circle is distorted, as

shown in the example of Fig. 10(b). The slope of the tangent to the locus of $Z_c(g_m)$ is increased in the vicinity of the imaginary axis, which significantly degrades the stability even with values of C_0 much larger than C_1 and C_2. The preferred solution uses a single transistor biased by a current source.

Using a fixed bias current requires sufficient margin to ensure oscillation with the maximum value of R (minimum Q) and for extreme values of process and environment corresponding to minimum transconductance. This increases the power consumption and gives a transconductance much higher than its critical value for the opposite extreme situation, which may drastically degrade the frequency stability through nonlinear effects. On the contrary, amplitude regulation at a low level through a feedback loop that adjusts the bias current virtually eliminates all nonlinear effects. It also limits the current just above its critical value in normal operation, while allowing a much larger start-up current to reduce the start-up time.

Except when a large amplitude of oscillation is accepted, an interface amplifier is necessary to produce a logic signal. This interface should not add too much loss in the oscillator. It should be optimized with respect to power consumption.

IV. Example of Practical Implementation

The circuit described here as an example of a high-performance oscillator is intended for a high-quality miniaturized 2-MHz ZT resonator [22], which provides a frequency stability within 10 ppm from -10 to 50°C. Its application in a watch requires a nominal current drain below 1 μA, and a minimum supply voltage of 1.1 V. Frequency adjustment is carried out digitally in the frequency-divider chain [23], so that no trimming is necessary in the oscillator. The complete diagram of the whole oscillator is shown in Fig. 11.

The heart of the oscillator uses transistor M_1 in a grounded source configuration, with the resonator connected to Q_1 and Q_2. It is biased by current I_0 delivered from an amplitude regulator. Transistor M_{17} is operated in weak inversion as a resistor, instead of lateral diodes in the polycrystalline silicon layer which were used in previous implementations [11], [24]. This resistor that forces M_1 into the active mode must have a very high value to avoid degrading the frequency stability and increasing the current. Its value is imposed at about 100 MΩ by the biasing transistors M_{15} and M_{19} matched to M_1 and M_{17} [10]. The total values of functional capacitors C_1 and C_2 (which include all stray capacitances at nodes Q_1 and Q_2) are selected to ensure a negligible influence of the voltage-dependent junction capacitances, without pushing the current too high.

The amplitude regulator is based on a known circuit [10], [25] in which high-value resistors are again implemented by M_{37} and M_{39} biased by M_7 and M_9. In the absence of oscillation, the regulator behaves as a current reference [10] which delivers a start-up current to the oscillator

$$I_{0\,\mathrm{start}} = A\frac{U_T}{R_7}\ln(K) \tag{35}$$

where K is the low current gain of loop M_3-M_6 and A is the ratio of mirror M_6, M_2. When the oscillation grows, I_0 decreases until the amplitude $|V_1|$ at node Q_1 reaches a value solely determined by K and nU_T, if M_3 and M_5 are in weak inversion. This amplitude can be adjusted to any higher value by the capacitive divider C_7, C_{11}. The choice of $|V_1|$ results from the optimum trade-off between the current consumption of the oscillator itself and that due to the output amplifier, including its loading of the oscillator.

The output amplifier and the following frequency-divider stages (not shown) are powered at a reduced voltage V_N to lower their current drain. The amplifier is a simple CMOS inverter M_{13}, M_{14} biased in active mode by the matched inverter M_{11}, M_{12} and by M_{23}. It uses concentric transistors to provide the maximum switching current with minimum size devices. It is capacitively coupled to node Q_1 of the oscillator. The total gate-to-drain capacitance C_M of M_{13} and M_{14} causes an input conductance G_1 to load the oscillator, which can be evaluated as follows, with reference to the ac equivalent circuit of Fig. 12. If load capacitance $C_L \gg C_M$, the gain of the amplifier is imaginary with

$$V_L = j\frac{|V_L|}{|V_1|}V_1. \tag{36}$$

If the gain is large, the complex input current is simply

$$I_1 = -j\omega C_M V_L. \tag{37}$$

Assuming that the output amplitude just reaches $V_N/2$, the combination of these equations yields

$$G_1 = I_1/V_1 = \omega C_M\frac{V_N}{2|V_1|}. \tag{38}$$

This conductance is inversely proportional to the oscillator amplitude $|V_1|$, which explains the trade-off in the choice of this amplitude.

The reduced voltage V_N is supplied by a dc voltage regulator which uses M_{21} and M_{22} matched to M_{11}, M_{12} and M_{13}, M_{14} as a reference delivering voltage V_R, and an adaptive biasing amplifier $M_{24}-M_{35}$ [26]. The input pair M_{33}, M_{35} of this amplifier operates in weak inversion. A critical amount of positive feedback is obtained by choosing a current gain of 2 through mirrors M_{26}, M_{24} and M_{25}, M_{27}. The output current I_L is then given by

$$\frac{I_L}{I_p} = \frac{B}{\exp\left(\dfrac{|V_N|-|V_R|}{nU_T}-1\right)} \tag{39}$$

where B is the ratio of mirror M_{26}, M_{32}. This relation is

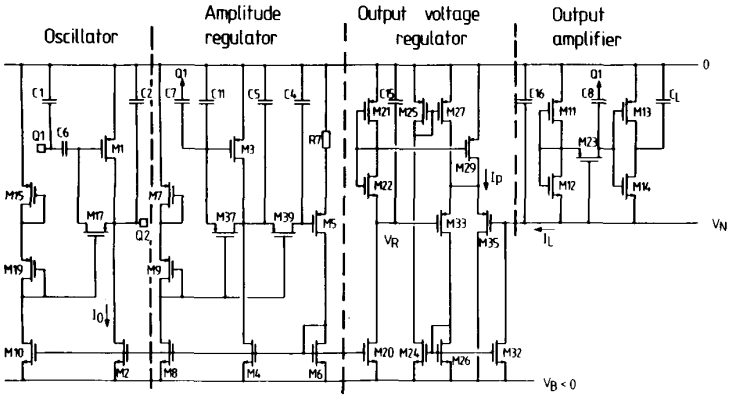

Fig. 11. Complete circuit diagram of the high-performance crystal oscillator.

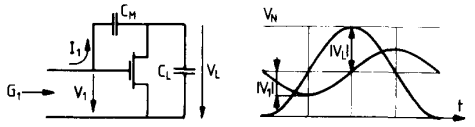

Fig. 12. Effect of Miller capacitor C_M of the output amplifier.

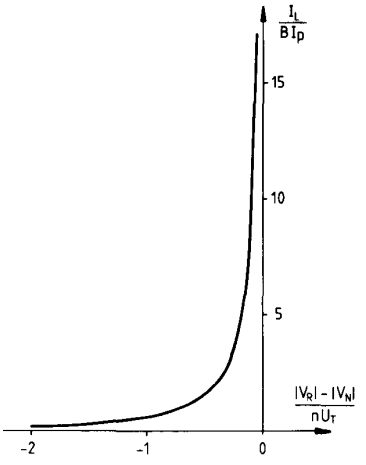

Fig. 13. Loading characteristics of the dc voltage regulator.

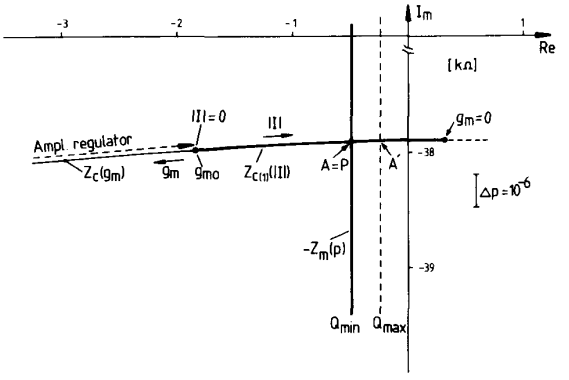

Fig. 14. Complex plane representation for the experimental oscillator.

plotted in Fig. 13, which shows that this voltage-follower amplifier achieves a very small offset $|V_R|-|V_N|$ for $I_L \gg BI_p$. The scaling current I_p mirrored by M_{29} is proportional to current I_0 in M_1. A high current efficiency is obtained by choosing a large value of mirror ratio B.

The calculated values for the oscillator based on Section III are given in Table I. They correspond to the complex plane representation of Fig. 14, which shows the relevant part of the circular locus of $Z_c(g_m)$ with its intersections A and A' with $-Z_m(p)$ for minimum and maximum values of Q. The influence of Q on frequency is obviously negligible. The amplitude regulation moves the value of g_m from its value for $I_{0\text{start}}$ (outside the plot) to small-signal value g_{m0}. The rest of the reduction to $g_{m\,\text{crit}}$ is due to nonlinear effects as discussed in Section III-C.

The influence of nonlinearities on frequency can in principle be calculated by computing $Z_{c(1)}(|I|)$ by the method presented in Section II-D, using SPICE for time-domain simulation and Fourier analysis. However, this influence is so small in this almost linear case that the computing accuracy is not sufficient to produce any valid

TABLE I
RESULTS OF CALCULATIONS FOR NOMINAL VALUES (BUT FOR EXTREMES OF R AND Q) AT 300 K

	Symbol	Figure Formula	Value	Unit
Crystal resonator				
Frequency	$\omega/2\pi$	(2)	2.1	MHz
Motional capacitance	C	Fig.1	.53	fF
Parallel capacitance	C_{12}	Fig.1	.55	pF
Motional resistance	R	Fig.1	240-480	Ohms
Quality factor	Q	(3)	600-300	10^5
Circuit				
Functional capacitances	C_1	Fig.5	2.8	pF
(including parasitics)	C_2	Fig.5	2.8	pF
Total parallel capacitance	C_3	Fig.6	.6	pF
Frequency pulling	p	(21)	133	10^{-6}
Critical transconductance	g_{mcrit}	(11+15)	1.60-2.27	μA/V
Critical current	I_{0crit}	(28)	67-95	nA
Amplitude of oscillation	$\|V_1\|$	Fig.6	300	mV
Bias current of M_1	I_0	Fig.9	258-396	nA
Start-up current in M_1	I_{0start}	(35)	960	nA
Current in oscil.+regulator		$4I_0/3$	344-488	nA
Total current with dividers			826-970	nA

TABLE II
EXPERIMENTAL RESULTS

Area on chip (complete oscillator)	.21mm^2
Total current (dividers unloaded)	.9uA at 1.5V
Minimum supply voltage	1.1V
Frequency dependence on voltage (1.1 to 5V)	.05ppm/V
Frequency instability in -10 to 60 C:	
Global with resonator	±10ppm
Contribution of circuit	<.1ppm

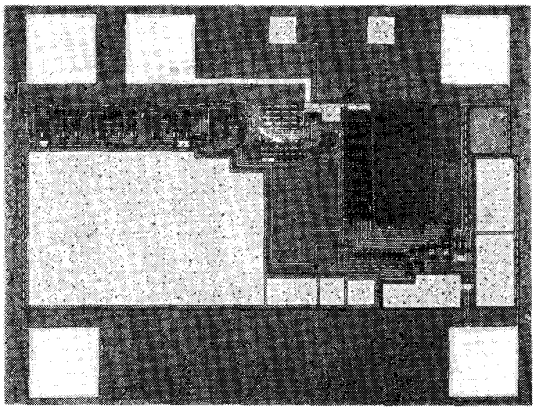

Fig. 15. Photomicrograph of the chip that combines the complete oscillator with a three-stage dynamic frequency divider.

result (accuracy should be better than 0.1 percent). In fact, $Z_{c(1)}(|I|)$ is superimposed on $Z_c(g_m)$, as shown on the same plot for $Q_{\min}$, and the nonlinear equilibrium point P falls almost exactly on linear point A. Nonlinear effects on frequency are thus completely negligible. This would not be the case if g_{m0} were much larger (no amplitude regulation) with a smaller diameter of the circle (large value of parallel capacitance C_3).

The circuit has been realized in the 3-μm p-well low-voltage SACMOS process [27]. The experimental chip shown in Fig. 15 includes three stages of dynamic frequency dividers. Its measured characteristics are reported in Table II. The measured frequency variation with temperature is virtually the same as that of the resonator alone. The current consumption falls within the calculated range. About half of it is due to the output amplifier and to the frequency divider.

This circuit has been implemented as module of a program for automatic synthesis of analog functional blocks, which allows it to be adapted to any set of specification in any technology [28].

V. CONCLUSION

Taking advantage of the very high Q of the resonator, the splitting of a crystal oscillator into the motional impedance Z_m of the resonator and the impedance Z_c of the rest of the circuit allows a detailed analysis of all linear and nonlinear effects to be carried out. It also provides the necessary insight to synthesize optimum solutions with respect to frequency stability and power dissipation. In the special case of single-transistor circuits (three-point oscillator), the linear analysis is simplified by the fact that Z_c is a bilinear function of the transconductance, which corresponds to a circular locus. The practical CMOS implementation presented as an example uses a robust amplitude regulator to limit the current below 1 μA at 2 MHz. It achieves a circuit stability better than 10^{-7} with voltage and temperature variations. The nonlinear analysis was only used in this case to help eliminate nonlinear effects; it is presently applied with success to less optimum situations.

ACKNOWLEDGMENT

The authors would like to thank F. Nicolas for analyzing the controlled-current CMOS inverter and L. Astier for computing the complex plane representation of the practical realization.

REFERENCES

[1] C. Fonjallaz and E. Vittoz, "Circuits électroniques pour montres-bracelet à quartz," in *Proc. Int. Congress Chronometry* (Paris, France), 1969, pp. B244-1 to 11.
[2] J. P. Moreau *et al.*, "Perfectionnement aux oscillateurs à quartz," French Patent Appl. 2 126 956, 1971.
[3] J. Luescher, "Circuit oscillateur à quartz à résonance parallèle, pour appareils de mesure du temps," Swiss Patent 504 039, 1971.
[4] S. S. Eaton, "Micropower crystal-controlled oscillator design using RCA COS/MOS inverter," RCA, Appl. Note ICAN-6539 1971.
[5] E. Vittoz, "Circuit d'entretien d'un oscillateur," Swiss Patent 532 336, 1972.
[6] M. P. Forrer, "Survey of circuitry for wrist-watches," *Proc. IEEE*, vol. 60, pp. 1047–1054, Sept. 1972.
[7] R. Tourki, "L'oscillateur à quartz en technologie CMOS," Ph.D. dissertation, Faculté des Sciences d'Orsay, Orsay, France, 1973.
[8] S. S. Chuang and E. E. Burnett, "Analysis of CMOS quartz oscillators," in *Proc. 9th Int. Congress Chronometry* (Stuttgart, W. Germany), Sept. 1974, paper C2.2.
[9] E. Vittoz, "LSI in watches," in *Proc. ESSCIRC* (Toulouse, France), 1976; full paper in *Solid State Circuits 1976*. Paris: Journal de Physique, pp. 7–27; also in *Pulse*, pp. 14–20, June 1978.
[10] E. Vittoz and J. Fellrath, "CMOS analog integrated circuits based on weak inversion operation," *IEEE J. Solid-State Circuits*, vol. SC-12, pp. 224–231, June 1977.
[11] E. Vittoz, "Quartz oscillators for watches," in *Proc. Int. Congress Chronometry* (Geneva, Switzerland), 1979, pp. 131–140.
[12] E. Vittoz, "Micropower IC's," in *Dig. ESSCIRC* (Paris, France), 1980, pp. 174–189.
[13] J. Luescher and A. Rusznyak, "A 4.2 MHz quartz oscillator for watch application," *Bull. SEV/ASE*, vol. 73, pp. 108–112, 1982.
[14] R. G. Meyer and D. C.-F. Soo, "MOS crystal oscillator design," *IEEE J. Solid-State Circuits*, vol. SC-15, pp. 222–228, Apr. 1980.
[15] M. A. Unkrich and R. G. Meyer, "Conditions for start-up in crystal oscillators," *IEEE J. Solid-State Circuits*, vol. SC-17, pp. 87–90, Feb. 1982.
[16] J. T. Santos and R. G. Meyer, "A one-pin crystal oscillator for VLSI circuits," *IEEE J. Solid-State Circuits*, vol. SC-19, pp. 228–236, Apr. 1984.
[17] A. Rusznyak, "Start-up time of CMOS oscillators," *IEEE Trans. Circuits Syst.*, vol. CAS-34, pp. 259–268, Mar. 1987.
[18] B. Parzen, *Design of Crystal and Other Harmonic Oscillators*. New York: Wiley, 1983.
[19] M. E. Frerking, *Crystal Oscillator Design and Temperature Compensation*. New York: Van Nostrand Reinhold, 1978.
[20] M. Wiegang, "Einige Ueberlegungen zur Dimensionierung von CMOS-Pierce-Oszillatoren," *Frequenz*, vol. 41, pp. 54–59, 1987.
[21] V. Uzunoglu, *Semiconductor Network Analysis and Design*. New York: McGraw Hill, 1964, p. 245.

[22] J. W. Hermann, "A novel miniature ZT-cut resonator," in *Proc. 39th Annual Symp. Frequency Control*, May 1985, pp. 375–380.
[23] E. Vittoz *et al.*, "Logical circuit for the wrist watch," in *Proc. Eurocon '71* (Lausanne, Switzerland), paper F 2-6.
[24] M. Dutoit and F. Sollberger, "Lateral polysilicon p-n diodes," *J. Electrochem. Soc.* vol. 125, pp. 1648–1651, Oct. 1978.
[25] E. Vittoz, "Micropower SC oscillator," *IEEE J. Solid-State Circuits*, vol. SC-14, pp. 622–624, June 1979.
[26] M. G. Degrauwe *et al.*, "Adaptive biasing CMOS amplifiers," *IEEE J. Solid-State Circuits*, vol. SC-17, pp. 522–528, June 1982.
[27] R. Luscher and J. S. De Saldivar, "A high density CMOS process," in *ISSCC Dig. Tech. Papers* (New York, NY), 1985, pp. 260–261.
[28] M. Degrauwe *et al.*, "An analog expert design system," in *ISSCC Dig. Tech. Papers* (New York, NY), 1987, pp. 212–213.

Eric A. Vittoz (A'63–M'72–SM'87) was born in Lausanne, Switzerland, on May 9, 1938. He received the M.S. and Ph.D. degrees in electrical engineering from the Federal Institute of Technology in Lausanne, Switzerland (EPFL) in 1961 and 1969, respectively.

After spending one year as a Research Assistant, he joined the Centre Electronique Horloger S.A. (CEH), Neuchâtel, Switzerland, in 1962, where he became involved in micropower integrated circuit developments for watches, while preparing a thesis in the same field. In 1971 he became Vice-Director of CEH, supervising advanced developments in electronic watches and other micropower systems. Since 1984 he has been Director of Centre Suisse d'Electronique et de Microtechnique S.A. (CSEM), in charge of the Division of Circuits and System Design. His field of personal research interest is the design of low-power analog circuits in CMOS technologies. Since 1975 he has also been lecturing and supervising student work in integrated circuit design at EPFL, where he became Titular Professor in 1982.

Marc G. R. Degrauwe (S'78–M'84) was born in Brussels, Belgium, on August 16, 1957. He received the engineering degree in electronics and the Ph.D. degree in applied sciences from the Katholieke Universiteit Leuven (KUL), Leuven, Belgium, in 1980 and 1983, respectively.

During the summer of 1980, he was on leave at Centre Electronique Horloger S.A. (CEH), Neuchâtel, Switzerland. From autumn 1980 to 1983, he was associated with KUL where he worked on the design of micropower amplifiers and sampled data filters. In July 1983 he returned to CEH. In 1984, when CEH was reorganized into the Swiss Centre of Electronics and Microtechnics (CSEM), he became Head of the Circuits Department. His actual field of interest is design automation of analog circuits. He is also lecturing on analog circuit design at the University of Neuchâtel.

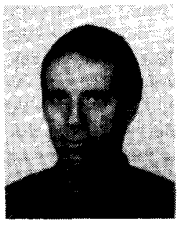

Serge Bitz was born in Sion, Switzerland, on November 30, 1959. He received the M.S. degree in electrical engineering from the Swiss Federal Institute of Technology (ETHZ), Zurich, in 1985.

He joined the Centre Suisse d'Electronique et de Microtechnique S.A. (CSEM), Neuchâtel, Switzerland, in 1985. Since then he has been engaged in the research and development of CMOS analog integrated circuits.